Modelling non-uniform strain distributions in aerospace composites using fibre Bragg gratings

Rajabzadehdizaji, Aydin; Groves, Roger M.; Hendriks, Richard C.; Heusdens, Richard

DOI
10.1117/12.2265376

Publication date
2017

Document Version
Final published version

Published in
Proceedings - 25th International Conference on Optical Fiber Sensors

Modelling non-uniform strain distributions in aerospace composites using fibre Bragg gratings

Aydin Rajabzadeh[a,b], Roger M. Groves[b], Richard C. Hendriks[a], and Richard Heusdens[a]

[a]Circuits and Systems Group, Delft University of Technology, The Netherlands
[b]Aerospace NDT Laboratory, Delft University of Technology, The Netherlands

ABSTRACT

In this paper the behaviour of fibre Bragg grating (FBG) sensors under non-uniform strain distributions was analysed. Using the fundamental matrix approach, the length of the FBG sensor was discretised, with each segment undergoing different strain values. FBG sensors that are embedded inside composites, also undergo such non-uniform strain distributions, when located in the vicinity of failures such as matrix cracks or delamination of layers. This non-uniform strain distribution was created in an experimental setup. Finite element analysis was used to analytically model the strain distribution along the FBG length. The measured FBG outputs were then compared to the simulated results. There was a high amplitude correlation between the results of the measured and the simulated reflection spectra with a maximum of 0.97 among all cases.

Keywords: FBG simulation, non-uniform strain, reflection spectra, structural health monitoring (SHM), fibre Bragg gratings, fundamental matrix method

1. INTRODUCTION

Fibre Bragg grating sensors have attracted a lot of attention in the field of structural health monitoring (SHM), during the past decades. The primary application of these sensors in SHM applications is for load monitoring and determining the absolute strain and temperature changes, either separately [1] or simultaneously [2]. Due to their often linear wavelength shift response, changes in average strain and temperature would result in a change in the position of the resonance wavelength of the FBG output [3]. However, the strain (or temperature) field affects the full reflection spectra of the sensor output signal. In this paper, the effects of strain distribution changes along the length of FBG sensors, and their effects on the reflection spectra's shape and wavelength shift were experimentally analysed. The composites of interest in this paper are mostly the continuous fibre-reinforced type, in which layers of reinforcing fibres are stacked in a desired configuration and FBG sensors could be embedded between these layers. The most prevalent types of damages in such composites are matrix cracks and delamination of layers. If there is contact between these cracks or openings with the FBG sensors, there would be a non-uniform strain distribution along the length of the FBG which would result in a alterations in its shape of reflected spectra [4]. In the next section the theory behind the FBG reflected spectra modelling is going to be described, the experimental design and results are discussed in section 3, and finally, section 4 concludes the paper.

2. THEORY

A fibre Bragg grating is a type of device that due to having a periodic (or aperiodic) perturbation in the refractive index of its core (called gratings), reflects particular wavelengths of light and transmits all other wavelengths. The highest reflection occurs at a certain wavelength called Bragg wavelength, calculated using equation (1):

$$\lambda_B = 2n_{eff}\Lambda \tag{1}$$

In which n_{eff} is the effective refractive index of the grating and Λ is the grating period.

Further author information:
E-mail: {A.Rajabzadehdizaji, R.M.Groves, R.C.Hendriks, R.Heusdens}@tudelft.nl

25th International Conference on Optical Fiber Sensors, edited by Youngjoo Chung, Wei Jin, Byoungho Lee, John Canning, Kentaro Nakamura, Libo Yuan, Proc. of SPIE Vol. 10323, 103237T · © 2017 SPIE · CCC code: 0277-786X/17/$18 · doi: 10.1117/12.2265376

In one of the earliest works of modelling the FBG reflection spectra, Yamada and Sakuda [5] proposed a piecewise-uniform approach, in which the length of the grating (L) is divided into a series of small segments (Δz), each assumed to act as independent uniform gratings. If the forward and backward fields for a segment i were defined as A_i and B_i, and assuming the starting point of $A_0 = A(L) = 1$ and $B_0 = B(L) = 0$, the coupled mode equations of field amplitudes for each segment could be solved as follows [5]:

$$\begin{pmatrix} A_i \\ B_i \end{pmatrix} = F_i \begin{pmatrix} A_{i-1} \\ B_{i-1} \end{pmatrix} \tag{2}$$

with

$$F_i = \begin{pmatrix} cosh(\gamma\Delta z) - j\frac{\Delta\beta}{\gamma} sinh(\gamma\Delta z) & -j\frac{\kappa}{\gamma} sinh(\gamma\Delta z) \\ j\frac{\kappa}{\gamma} sinh(\gamma\Delta z) & cosh(\gamma\Delta z) + j\frac{\Delta\beta}{\gamma} sinh(\gamma\Delta z) \end{pmatrix} \tag{3}$$

in which κ is the coupling coefficient between forward and backward waves, $\Delta\beta = 2\pi n_{\mathrm{eff}}(\frac{1}{\lambda} - \frac{1}{\lambda_\mathrm{B}})$ is the difference between propagation constants in the longitudinal direction in which n_{eff} is the effective refractive index, λ is the wavelength and λ_B is the initial Bragg reflection wavelength, and $\gamma = \sqrt{\kappa^2 - \Delta\beta^2}$. After calculating the F_i matrix for each segment, the desired backward and forward output amplitudes were derived using the relation:

$$\begin{pmatrix} A_M \\ B_M \end{pmatrix} = F \begin{pmatrix} A_0 \\ B_0 \end{pmatrix} \quad \text{in which} \quad F = F_M \cdot F_{M-1} \cdot \ldots \cdot F_1. \tag{4}$$

The reflected spectrum, $R(\lambda)$, is then determined as:

$$R(\lambda) = \left| \frac{B_M}{A_M} \right|^2. \tag{5}$$

As long as the segments are not that small and $\Delta z \gg \Lambda$, the results are sufficiently accurate.

3. PHYSICAL CASE

The process of applying a partial strain on the grating, could be considered similar to the case of delamination of composite layers, when the FBG is embedded between the layers and is in the vicinity of the opening section of the layers. It has been shown in the literature that depending on the location of delamination along the length of the FBG sensor, there could be an additional strain distribution in opening areas, either in the middle or on the two end parts of sensor [6].

For the sake of simplicity of implementation and avoiding undesired artefacts, only the "end region strain" was considered in this paper, and the experimental setup was designed accordingly. In order to have more control over the strain distribution along the length of the sensor, this case was simplified to the laboratory setup of Figure 1. In this setup an optical fibre with an overall length of one meter was used, in which a length of $L = 10\,mm$ contained gratings, with central wavelength of $\lambda_c = 1539.76\,nm$. In order to have a better comparison between the simulation results and the measured outputs, the data acquisition was divided into 9 sessions, with each session corresponding to 1 mm of grating length being covered in Cyanoacrylate type adhesive. In the first session, $1\,mm$ of the length of the grating was glued to a stiff surface (12 layer woven fabric CFRP composite of size 20 by 20 cm and thickness of $8\,mm$), with one end of optical fibre being connected to a PXIe-4844 FBG interrogator (with $4\,pm$ wavelength accuracy and wavelength range of $1510\,nm$ to $1590\,nm$), and the other end being connected to a mass of $200\,g$, which was responsible for applying stress on the FBG and creating the desired strain distribution. Data acquisition was performed afterwards, and then another $1\,mm$ of the length of the grating was covered and so forth. This process continues until the whole length of FBG is covered in glue.

Finite element analysis (FEA) was used to assess the strain distribution along the length of sensor. Quad type elements were chosen with sizes equal to the modelling segments, which were $\Delta z = 0.05\,mm$ in length. The

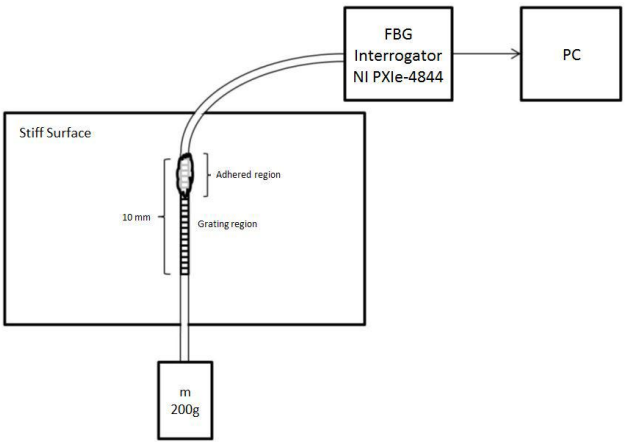

Figure 1: Laboratory setup for creating the non-uniform strain distribution along the length of an FBG sensor. Only the glued part of the optical fibre was attached to the surface and the rest of the fibre was loose.

(a) (b)

Figure 2: Finite element modelling of the optical fibre for the grating region (a) and the resulting strain distribution along its length (b) for the case of 3 mm adhesive coverage.

boundary conditions were zero displacement and rotation on the mutual surface of the stiff surface and the adhesive. Consequently, for the total of $M = 20$ FBG segments, there were 20 different strain values (and therefore 20 different wavelength shifts). The finite element modelling was performed in ABAQUS 6.14, and the modelled setup and strain distribution along the length of FBG sensor is shown in Figure 2. As you can see from the simulated strain values, the length that is covered in adhesive is under lower strain (similar to the area of sensor adhered to binding material in composites), and the rest of the sensor that is loose is under higher strain (similar to the length of the FBG sensor that is in the vicinity of an opening in delaminated composite). This strain distribution actually affects the $\Delta\beta$ and γ parameters in each of the F_i matrices differently, which in the end results in alteration of original reflection spectra of the FBG . In order to have a better view of the strain changes on the optical fibre, the glued region and also the surface were excluded from viewing. In order to visualise the comparison of our modelling with actual output measurements, the case of 3 mm covering of FBG length in adhesive is chosen to be presented here.

Based on the results of the FEA, the strain values were applied in the simulation code (generated in MATLAB 2016A). The modelled output and the measured output of the signal at 3 mm glue coverage of sensor are shown together in Figure 3. It can be observed that the shape of the modelled reflection spectra, complies significantly with the modelled output, and also with some output signals of delamination type damages in composites that were presented in the literature [6,7]. In fact, even though the real FBG sensors suffer from intrinsic manufacturing and drawing birefringence, the results of modelling and actual output measurements had a maximum of 0.97 correlation with each other (at 3 mm glue coverage). The calculated similarity of the measured and simulated signals, based on Pearson's sample correlation [8], are shown in Table 1.

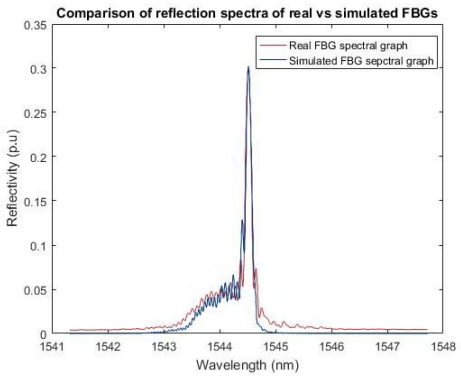

Figure 3: Reflection spectra for the measured and simulated FBG sensors. Due to the applied stress, there is an approximate of 5 nm wavelength shift on both simulated and measured reflection spectra.

Table 1: Correlation results between the simulated and real FBG output under similar strain distributions.

Covered length of FBG in adhesive (in mm)	1	2	3	4	5	6	7	8	9
Amplitude correlation	0.95	0.94	0.97	0.93	0.93	0.91	0.92	0.88	0.85

As it is seen from the table, the higher the length of FBG being covered in adhesive, the less correlated are the modelled output and the real FBG measurements. The reason is that adding more layers of adhesive created uneven distribution of adhesive on the sensor surface, which resulted in deviation of actual strain distribution from that of our simulations.

4. CONCLUSIONS

This paper shows the high correlation of the results, derived from modelling the FBG, and actual output measurements from a real FBG sensor in similar strain distributions. Although in many of the applications of FBGs in SHM, the focus is only on the peak resonance wavelength shifts, in many of the recent studies there has been an effort in exploiting the information in the full range of the reflection spectra, especially in damage classification and monitoring the damage growth. The primary goal of this experiment was to give a better understanding and intuition of the behaviour of FBG sensors under such strain distributions.

5. REFERENCES

[1] Rao, Y. J., "In-fibre Bragg grating sensors." Measurement science and technology 8(4), 355-375 (1997).
[2] Mizutani, Y., Groves, R. M., "Multi-Functional Measurement Using a Single FBG Sensor", Experimental mechanics 51(9), 1489-1498 (2011).
[3] Kashyap, R., [Fiber Bragg Gratings], Academic press, 142-157 (1999).
[4] Sorensen, L., Botsis, J., Gmur, T., and Cugnoni, J., "Delamination detection and characterisation of bridging tractions using long FBG optical sensors.", Composites Part A: Applied Science and Manufacturing 38(10), 2087-2096 (2007).
[5] Yamada, M. and, Sakuda, K., "Analysis of almost-periodic distributed feedback slab waveguides via a fundamental matrix approach." Applied optics 26(16), 3474-3478 (1987).
[6] Takeda, S., Minakuchi, S., Okabe, Y., and Takeda, N., "Delamination monitoring of laminated composites subjected to low-velocity impact using small-diameter FBG sensors", Composites Part A: Applied Science and Manufacturing 36(7), 903-908 (2005).
[7] Takeda, S., Yamamoto, T., Okabe, Y., Takeda, N., "Debonding monitoring of composite repair patches using embedded small-diameter FBG sensors", Smart materials and structures 16(3), 763-770 (2007).
[8] Sprent, P., and Smeeton, N. C. , [Applied nonparametric statistical methods (3rd ed.)]. CRC Press, 283-314 (2001).